Proceedings of the
IEEE Intelligent Vehicles Symposium 2000
Dearborn (MI), USA • October 3-5, 2000

Optimal trajectory planning with quintic G^2-splines.

Corrado GUARINO LO BIANCO and Aurelio PIAZZI
Dipartimento di Ingegneria dell'Informazione
Universitá di Parma
I-43100 Parma, ITALY
guarino@ce.unipr.it aurelio@ce.unipr.it

Abstract

This paper deals with the generation of optimal paths for the automated steering of autonomous vehicles. The path is parametrized by quintic G^2-splines, or η-spline, devised to guarantee the overall second order geometric continuity of a composite path interpolating an arbitrary sequence of points. Starting from the closed-form η-parametrization of the spline an optimization criterion is proposed to design smooth curves. The aim is to plan curves where the curvature variability is kept as small as possible. With good approximation, in a flatness based control scheme, this corresponds to minimize the change-rate of the steering control. Various examples are included to highlight the ductility and effectiveness of the planning.

1 Introduction.

The recent literature proposes various approaches to give an answer to the problem of the lateral control of autonomous vehicles. Considerable differences can be found between the solutions adopted. These differences are constituted, for example, by the several sensing devices adopted to detect the position of the vehicle with respect to the environment: guiding wires drowned under the road surface, microwave radars, visual servoing devices [5, 9, 4]. Another distinction is given by the type of control technique selected: a fuzzy logic approach was proposed by Hessburg and Tomizuka [7], robust controllers were proposed in [1, 3], neural networks were adopted and subsequently developed in the RALPH project [11]. A comparative survey on various vision-based control strategies for autonomous vehicles can be found in the paper of Taylor *et al.* [12].

In [2] we have proposed a novel control strategy based on the flatness properties of a simplified vehicle model. Succinctly, the controller computes the instantaneous steering angle required to follow a predefined curve on the basis of a dynamic inversion procedure. The approach is somehow similar to that proposed by Tsugawa *et al.* in [13] but in [2] we have shown that, to obtain continuous steering commands, the assigned curve must exhibit well defined geometric characteristics. To account this requirement, we have proposed to parametrize the curve by means of a new type of polynomial splines, i.e. the quintic G^2-splines. Their properties are shown and discussed in detail in [10]. The novel spline curves satisfy a second order geometric continuity requirement and, at the same time, introduce some degrees of freedom that can be spent to improve the quality of the trajectory planning. In this paper we will show how these degrees of freedom can be optimally used to obtain smooth steering commands to track at best the road lane.

In §2 a brief introduction to the mathematics of the planar curves is given. In the subsequent section the relevant optimization problem is proposed. Finally, the results of some optimizations are given in §4. In particular the optimal splines for a lane change and for some road curves are evaluated.

2 Preliminaries on planar curves.

The following definitions, derived from the theory of planar curves [8], will be used in the sequel of this paper.

The Euclidean norm of a vector $\mathbf{p}$ is denoted with $\|\mathbf{p}\|$. A generic point on the $\{x,y\}$-plane is indicated by the real vector $\mathbf{p} := [x\ y]^T \in \mathbb{R}^2$. A planar path, i.e. a set of points in the $\{x,y\}$-plane, is described by means of a vector function in the real parameter $u \in [u_0, u_1]$: $\mathbf{p}(u) := [x(u)\ y(u)]^T$. We consider $\mathbf{p}(u)$ as an oriented curve starting from $\mathbf{p}(u_0) := [x_A\ y_A]^T$ and ending in $\mathbf{p}(u_1) := [x_B\ y_B]^T$. Indicate by $\dot{\mathbf{p}}(u)$ the first derivative of $\mathbf{p}(u)$ with respect to u: $\dot{\mathbf{p}}(u) := [dx/du\ dy/du]^T$. A curve $\mathbf{p}(u)$ is "regular" if $\dot{\mathbf{p}}(u)$ is well defined over $[u_0, u_1]$ and $\dot{\mathbf{p}}(u) \neq 0\ \forall u \in [u_0, u_1]$. The curvilinear coordinate measured along the path $\mathbf{p}(u)$ is denoted by s; it can be computed as a function of u by means of

$$s = f(u) := \int_{u_0}^{u} \|\dot{\mathbf{p}}(\xi)\|\, d\xi. \tag{1}$$

For regular curves the inverse function $u = f^{-1}(s)$ is well defined. By virtue of $f(u)$ and its inverse, all subsequent

0-7803-6363-9/00/$10.00 © 2000 IEEE

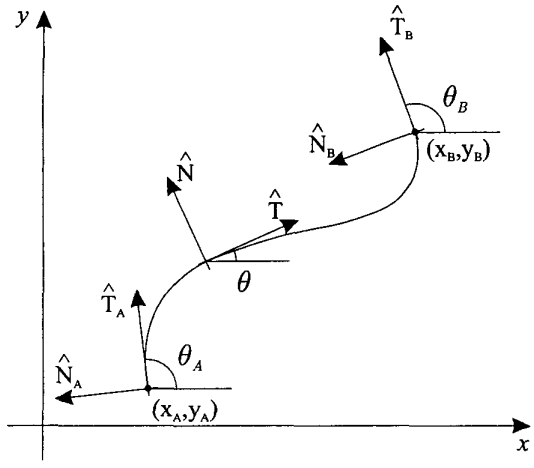

Figure 1: Frenet frames

equations can be expressed indifferently as functions of s or u.

According to the theory of planar curves, for each point $\mathbf{p}(u)$ we have a Frenet frame given by a couple of orthogonal unit vectors $\hat{T}(u)$ and $\hat{N}(u)$ (see Fig. 1). The unit vector $\hat{T}$ is tangent to the curve and its versus coincides with the curve orientation whereas the versus of $\hat{N}$ is arbitrary. In this paper $\hat{N}$ has been chosen in such a way $\{\hat{T},\hat{N}\}$ is congruent to the $\{x,y\}$ frame (see Fig. 1). A Frenet frame is completely defined by the description its origin ($\mathbf{p}(u)$) and its orientation (say $\theta(u)$) with respect to a fixed frame. Each Frenet frame satisfies the following equations

$$\frac{d\mathbf{p}}{ds} = \frac{\dot{\mathbf{p}}}{\|\dot{\mathbf{p}}\|} = \hat{T}, \quad \frac{d^2\mathbf{p}}{ds^2} = \frac{(\dot{\mathbf{p}}\times\ddot{\mathbf{p}})\times\dot{\mathbf{p}}}{\|\dot{\mathbf{p}}\|^4} = \kappa\hat{N}, \qquad (2)$$

where the scalar $\kappa(u)$ is the curvature of the path at $\mathbf{p}(u)$. The sign of $\kappa(u)$ is defined by the choice of $\hat{N}$. We indicate by κ_A and κ_B the curvature at the beginning and at the end of the path respectively. In the same way, we indicate by θ_A and θ_B the orientation of the Frenet frame at the curve endpoints.

A curve $\mathbf{p}(u)$ has first order geometric continuity, i.e. $\mathbf{p}(u) \in G^1$, if $\mathbf{p}(u)$ is regular and its unit tangent vector $d\mathbf{p}/ds$ is a continuous function over $[u_0,u_1]$. Moreover, a curve $\mathbf{p}(u)$ has second order geometric continuity, i.e. $\mathbf{p}(u) \in G^2$, if $\mathbf{p}(u) \in G^1$ and its curvature vector $d^2\mathbf{p}/ds^2$ is continuous over $[u_0,u_1]$ [8]. By natural extension we say that a $\{x,y\}$-path belongs to G^i, $i \in \{1,2\}$ if there exists a parametric curve $\mathbf{p}(u) \in G^i$ such that its image is the $\{x,y\}$-path.

3 The optimal quintic G^2-splines.

This paper is motivated by demands arisen form the flatness control strategy proposed in [2]. In that paper a dynamic inversion based control was proposed for the lateral motion of autonomous vehicles described by means of the simplified nonholonomic model

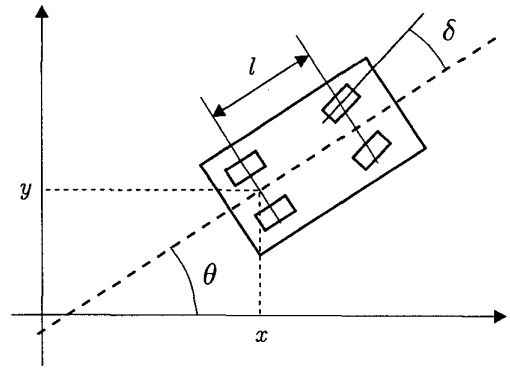

Figure 2: Vehicle's variables of the model (3).

$$\begin{cases} \dot{x} &= v\cos\theta \\ \dot{y} &= v\sin\theta \\ \dot{\theta} &= \frac{v}{l}\tan\delta \end{cases}, \qquad (3)$$

where v is the vehicle's (constant) velocity, l is the inter-axle distance, δ is the front wheel steering angle. The state variables x, y, and θ denote respectively the cartesian coordinates and the angular displacement of a frame affixed to the midpoint of the vehicle's rear axle (see fig. 2). In [2] it has been also demonstrated that it is possible to guide the vehicle along a prespecified path with a continuous control law $\delta(t)$ if and only if the geometric continuity of the path is, at least, of class two (G^2).

In a previous paper of the authors [10] quintic G^2-splines, or η-splines, are proposed to plan a composite G^2-path interpolating an arbitrary sequence of points. Closed-form expressions of the η-spline can be presented as follows ($u \in [0,1]$):

$$\mathbf{p}(u) = \begin{bmatrix} x(u) \\ y(u) \end{bmatrix} := \\ := \begin{bmatrix} x_0 + x_1u + x_2u^2 + x_3u^3 + x_4u^4 + x_5u^5 \\ y_0 + y_1u + y_2u^2 + y_3u^3 + y_4u^4 + y_5u^5 \end{bmatrix} \qquad (4)$$

where

$$\begin{aligned} x_0 &= x_A \\ x_1 &= \eta_1\cos\theta_A \\ x_2 &= \frac{1}{2}\left(\eta_3\cos\theta_A - \eta_1^2\kappa_A\sin\theta_A\right) \\ x_3 &= 10(x_B - x_A) - (6\eta_1 + \frac{3}{2}\eta_3)\cos\theta_A \\ &\quad -(4\eta_2 - \frac{1}{2}\eta_4)\cos\theta_B + \frac{3}{2}\eta_1^2\kappa_A\sin\theta_A - \frac{1}{2}\eta_2^2\kappa_B\sin\theta_B \\ x_4 &= -15(x_B - x_A) + (8\eta_1 + \frac{3}{2}\eta_3)\cos\theta_A \end{aligned}$$

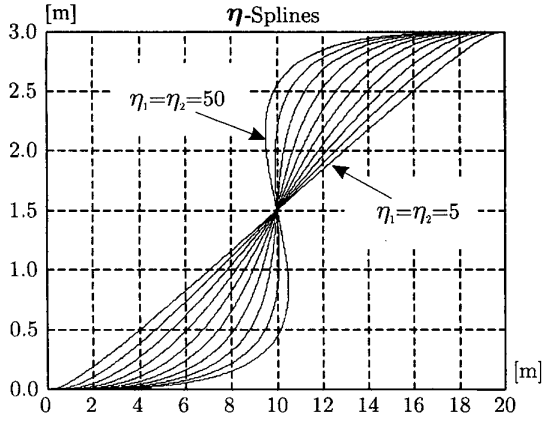

Figure 3: Lane change. ($\eta_3 = \eta_4 = 0$)

$$+(7\eta_2 - \eta_4)\cos\theta_B - \frac{3}{2}\eta_1^2\kappa_A\sin\theta_A + \eta_2^2\kappa_B\sin\theta_B$$

$$x_5 = 6(x_B - x_A) - (3\eta_1 + \frac{1}{2}\eta_3)\cos\theta_A$$

$$-(3\eta_2 - \frac{1}{2}\eta_4)\cos\theta_B + \frac{1}{2}\eta_1^2\kappa_A\sin\theta_A - \frac{1}{2}\eta_2^2\kappa_B\sin\theta_B$$

$$y_0 = y_A$$

$$y_1 = \eta_1\sin\theta_A$$

$$y_2 = \frac{1}{2}\left(\eta_3\sin\theta_A + \eta_1^2\kappa_A\cos\theta_A\right)$$

$$y_3 = 10(y_B - y_A) - (6\eta_1 + \frac{3}{2}\eta_3)\sin\theta_A$$

$$-(4\eta_2 - \frac{1}{2}\eta_4)\sin\theta_B - \frac{3}{2}\eta_1^2\kappa_A\cos\theta_A + \frac{1}{2}\eta_2^2\kappa_B\cos\theta_B$$

$$y_4 = -15(y_B - y_A) + (8\eta_1 + \frac{3}{2}\eta_3)\sin\theta_A$$

$$+(7\eta_2 - \eta_4)\sin\theta_B + \frac{3}{2}\eta_1^2\kappa_A\cos\theta_A - \eta_2^2\kappa_B\cos\theta_B$$

$$y_5 = 6(y_B - y_A) - (3\eta_1 + \frac{1}{2}\eta_3)\sin\theta_A$$

$$-(3\eta_2 - \frac{1}{2}\eta_4)\sin\theta_B - \frac{1}{2}\eta_1^2\kappa_A\cos\theta_A + \frac{1}{2}\eta_2^2\kappa_B\cos\theta_B.$$

Subscripts A and B indicate the assigned interpolating conditions relative to the spline endpoints, while $\boldsymbol{\eta} := [\eta_1\ \eta_2\ \eta_3\ \eta_4]^T \in \mathcal{H} := (0,+\infty)\times(0,+\infty)\times(-\infty,+\infty)\times(-\infty,+\infty)$ is a vector of free parameters. It is worth stressing that the interpolating conditions are always fulfilled for any $\boldsymbol{\eta} \in \mathcal{H}$. For more details concerning the characteristics of the G^2-splines see [10].

To show how $\boldsymbol{\eta}$ affects the shape of a curve let consider the lane changes ($\theta_A = \theta_B = 0$ and $\kappa_A = \kappa_B = 0$) plotted in Figs. 3 and 4.

In the first figure η_1 and η_2 are varied whereas η_3 and η_4 are constant ($\eta_3 = \eta_4 = 0$). Note $\eta_1 = \dot{\mathbf{p}}(0)$ and $\eta_2 = \dot{\mathbf{p}}(1)$ so that η_1 mainly influences the shape of the curve at the beginning while η_2 affects its closing. In general, high values for η_1 forces θ and κ to stay close to the initial values θ_A and κ_A for a long while. The parameter η_2 has analogous effects on the curve closing. To attain symmetric curves we have imposed $\eta_1 = \eta_2$. In Fig. 4, η_1 and η_2 are kept constant and curves are traced for different values of η_3 and η_4. This time, to obtain symmetric shapes, it is necessary to impose $\eta_3 = -\eta_4$ [10]. Parameters η_3 and η_4 modulate the curvature variation at the beginning and at the closing of the spline respectively. In Fig. 5 a detail of the curve closing is shown. Very positive values of η_4 cause strong curvature variations while approaching the end point. The parameter η_3 has a similar influence on the curve beginning but, this time, very negative values are required to cause a considerable curvature variability.

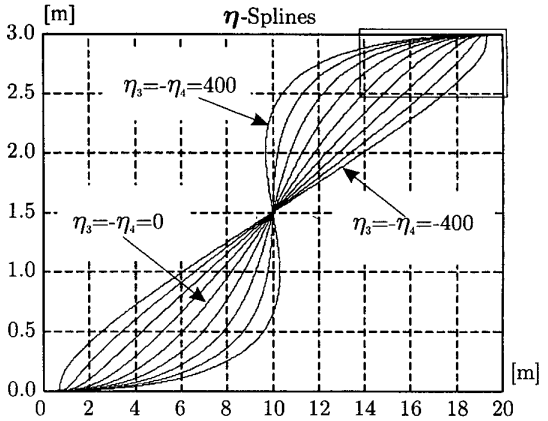

Figure 4: Lane change. ($\eta_1 = \eta_2 = 20$)

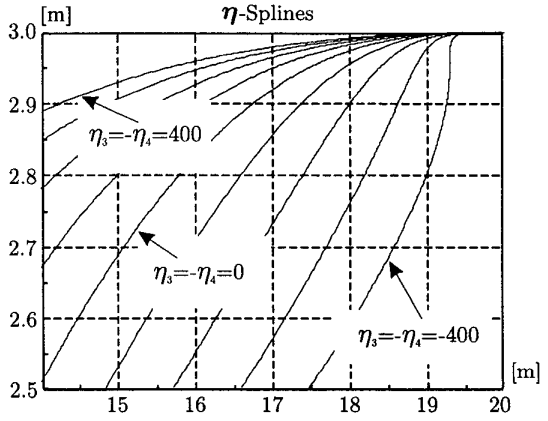

Figure 5: Detail of a lane change. ($\eta_1 = \eta_2 = 20$)

It is clear that, with a proper selection of $\boldsymbol{\eta}$, it is possible to obtain a wide number of shapes for the path, all of them satisfying the interpolating conditions at the curve extremes. This suggests to choose the four parameters according with some sort of optimality criterion. In this pa-

per we select them by minimizing $|d\kappa/ds|$ because, under reasonable approximations, it is equivalent to minimize the absolute value of the derivative of the steering angle δ with respect to time. Indeed, in determining the steering angle control with the flatness based approach [2, 10] we use the relation

$$\delta = \arctan(l\kappa) \tag{5}$$

where κ is the current curvature of the followed path. Hence we can express the first derivative of δ with respect to the time as follows

$$\frac{d\delta}{dt} = l\frac{d\kappa}{dt}\frac{1}{\arctan^2(l\kappa)+1}. \tag{6}$$

In many planning contexts, such as in road driving, small values of κ are typical so that it is a good approximation to consider $d\delta/dt$ proportional to $d\kappa/dt$ and minimize this latter to reduce the change-rate of δ. On the other hand, the path curvature κ depends on curvilinear coordinate s so that we can write

$$\frac{d\kappa}{dt} = \frac{d\kappa}{ds}\frac{ds}{dt} = \frac{d\kappa}{ds}v \tag{7}$$

where v is the vehicle's velocity. Since v is considered constant (at least while travelling along a single spline) it follows that the variability of the steering angle can be indirectly reduced by minimizing the maximum of $|d\kappa/ds|$ along the whole path. Thus, the optimization problem can be formulated as follows

$$\min_{\eta\in\mathcal{H}} \max_{s\in[0,f(1)]} \left|\frac{d\kappa}{ds}(s)\right| \tag{8}$$

or, equivalently, by considering (1)

$$\min_{\eta\in\mathcal{H}} \max_{u\in[0,1]} \left|\frac{d\kappa}{ds}(u)\right| \tag{9}$$

subject to

$$\|\dot{\mathbf{p}}(u)\| > 0 \qquad \forall u \in [0,1]. \tag{10}$$

The constraint (10) has been added to guarantee the regularity of the curve (see [10] on the regularity issue). The minimax problem (9) can be converted into a semi-infinite problem by adding to vector η an auxiliary variable η_5: $\tilde{\eta} := [\eta^T\ \eta_5]^T \in \tilde{\mathcal{H}} := \mathcal{H} \times [0,+\infty)$. The optimization problem then becomes

$$\min_{\tilde{\eta}\in\tilde{\mathcal{H}}} \eta_5 \tag{11}$$

subject to

$$\left|\frac{d\kappa}{ds}(u)\right| \le \eta_5 \qquad \forall u \in [0,1]; \tag{12}$$

$$\|\dot{\mathbf{p}}(u)\| > 0 \qquad \forall u \in [0,1]. \tag{13}$$

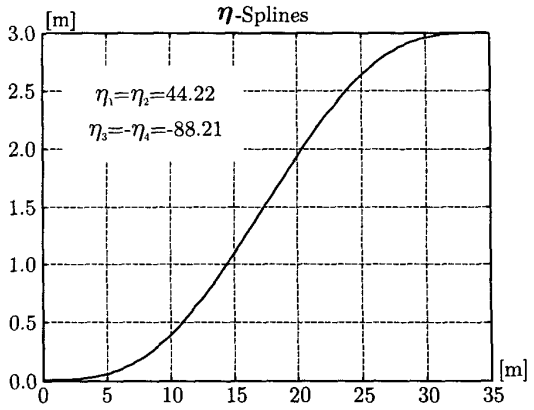

Figure 6: Optimal lane change.

An useful expression for $d\kappa/ds$ can be deduced as follows (see (1)):

$$\frac{d\kappa}{ds} = \frac{d\kappa}{du}\frac{du}{ds} = \frac{d\kappa}{du}\Big/\frac{ds}{du} = \frac{d\kappa/du}{\|\dot{\mathbf{p}}\|}. \tag{14}$$

The actual solution of the above semi-infinite optimization problem can be pursued with local techniques such as, for example, Sequential Quadratic Programming, or with the hybrid genetic/interval algorithm of Guarino and Piazzi [6] aimed to obtaining an estimate of the global solution.

In real time applications suboptimal values for η could be obtained by look-up tables previously constructed with extensive off-line programming.

4 Illustrative examples.

In this section, we test the capability of the G^2-splines to approximate realistic road paths. Three different cases will be considered. In the first case, an optimal path for a lane change is generated. The second and the third examples check the capability of the G^2-splines to approximate some actual road profiles: a circular arch and a clothoid arch. In all the three cases the vehicle path has been generated by solving the optimization problem described in §3, i.e. by minimizing the curvature variability. The adopted optimization solver is the hybrid algorithm presented in [6].

In the first example a lane change along a straight road is considered. The path starts from the origin of the reference frame and ends at $x_B = [35\ 3]^T$. The initial and the final angles and curvatures are equal to zero ($\theta_A = \theta_B = 0, \kappa_A = \kappa_B = 0$). The obtained optimal solution is given by $\eta = [44.22\ 44.22\ -88.21\ 88.22]^T$. The corresponding path is shown in Fig. 6 while its curvature and first derivative are shown in Fig. 7.

In the second experiment the input data for the G^2-splines are derived from circular arches (see Tab. 1). Three different radius are considered. The curves start again from the

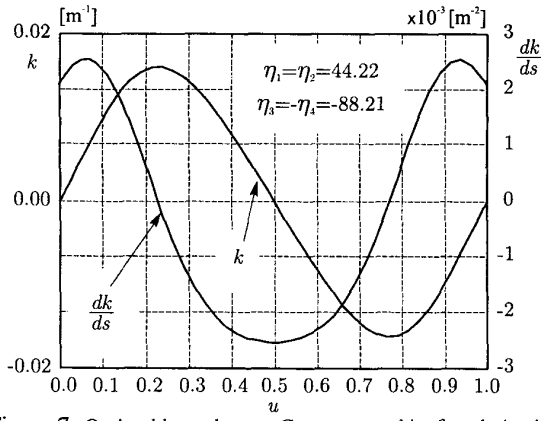

Figure 7: Optimal lane change. Curvature and its first derivative with respect to s of the optimal path.

Table 1: Parameters for the circular curves.

radius	50 m	200 m	2000 m
$x_A = y_A$ [m]	0	0	0
x_B [m]	32.21	34.82	35.00
y_B [m]	11.76	3.055	0.31
θ_A [rad]	0	0	0
θ_B [rad]	0.7	0.175	0.0175
$k_A = k_B$ [m^{-1}]	1/50	1/200	1/2000

origin of the reference frame with an initial angle equal to zero radians. The endpoint data are derived by considering circular arches with a length equal to 35 m. The initial and the final curvatures are supposed to be equal to the reciprocal of the curve radius. It is clear that, owing to these choices, if the G^2-splines are able to generate approximate circular arches, the obvious solution of the optimization problem is given by curves where $\kappa(u) \cong \kappa_A = \kappa_B$ for all $u \in [0,1]$. Indeed, this guarantees that $d\kappa/ds \cong 0$. The obtained optimal G^2-spline curves are plotted upon actual circular curves in Fig. 8. In all the cases the optimal solution is given by $\eta_1 = \eta_2 = 35$ (i.e. the curve length) and $\eta_3 = \eta_4 = 0$. As desired, $d\kappa/ds$ is very close to zero. Its maximum absolute value is equal to $1.0841 \cdot 10^{-6}$ when the radius is equal to 50 m and decreases to $8.1957 \cdot 10^{-7}$ and $1.1341 \cdot 10^{-14}$ when the radius is equal to 200 and 2000 m respectively. The corresponding curvatures and their first derivatives are shown in Fig. 9.

In the last experiment we attempted to approximate some clothoid curves by means of the G^2-splines. The starting point and angle are the same considered for previous examples but the initial curvature is supposed to be zero. The endpoint x_B and the final angle θ_B are evaluated by considering a 35 m long clothoid arch and three different values for the final curvature (see Tab. 2). In this case the obvious solution requires $\kappa(s)$ to be linearly increasing with respect

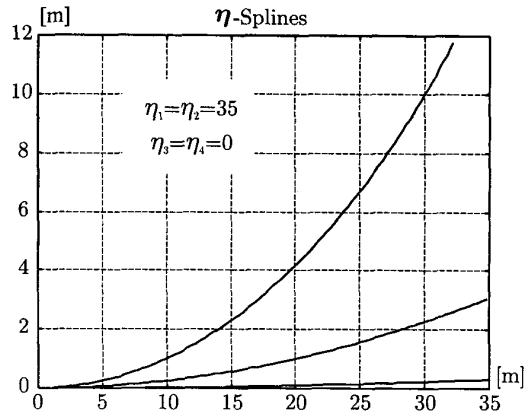

Figure 8: Optimal spline arches for three different curvatures ($k = \{20 \cdot 10^{-3}, 5 \cdot 10^{-3}, 0.5 \cdot 10^{-3}\}$). Actual circular arches, drawn over the spline arches, cannot be distinguished.

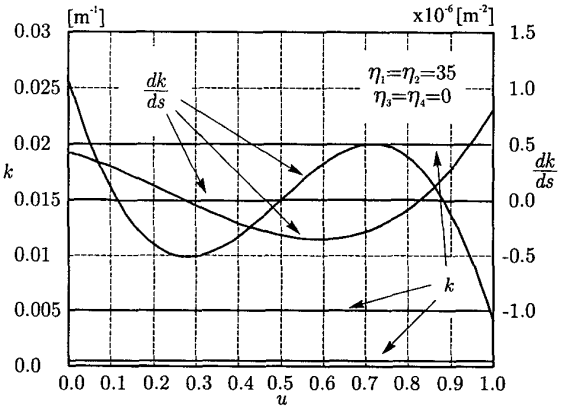

Figure 9: Curvature and its first derivative with respect to s for the three spline arches. In all the cases curvature is almost constant along the whole path.

to s so that $|d\kappa/ds|$ is constant and equal to the minimum value. Note that if $\kappa(s)$ is linearly increasing we are implicitly planning clothoid curves. Also in this case the optimal solution obtained, $\eta = [35\ 35\ 0\ 0]^T$, is characterized with a neat symmetry. In Fig. 10 the optimal solutions are compared with actual clothoids while their curvatures and first derivatives are shown in Fig. 11. As desired, the curvature derivatives are almost constant. The largest value relates to a final curve radius equal to 50 m: in that case $\eta_5 = 5.9149 \cdot 10^{-4}$. Smaller derivatives are obtained in the other two cases: $1.4317 \cdot 10^{-4}$ and $1.4286 \cdot 10^{-5}$ for a final radius equal to 200 and 2000 m respectively.

5 Conclusions.

An optimal trajectory planning using quintic G^2-splines is proposed to minimize the change-rate of the curvature. The examples proposed also show how the G^2-splines can

Table 2: Parameters for the clothoid curves.

Final radius	50 m	200 m	2000 m
$x_A = y_A$ [m]	0	0	0
x_B [m]	34.57	34.97	35.00
y_B [m]	4.05	1.02	0.10
θ_A [rad]	0	0	0
θ_B [rad]	0.35	0.0875	$8.75 \cdot 10^{-3}$
k_A [m^{-1}]	0	0	0
k_B [m^{-1}]	1/50	1/200	1/2000

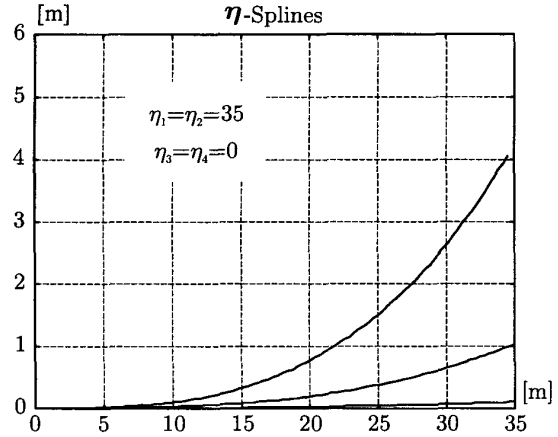

Figure 10: Optimal spline clothoids for three different final curvatures $k = \{20 \cdot 10^{-3}, 5 \cdot 10^{-3}, 0.5 \cdot 10^{-3}\}$. Actual clothoids, drawn over the spline clothoids, cannot be distinguished.

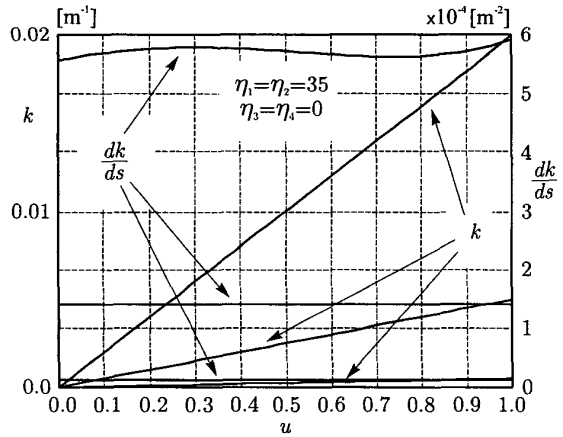

Figure 11: Curvature and its first derivative with respect to s for the three spline clothoids. In all the cases, the curvature increases almost linearly along the whole path.

be used to approximate a significant variety of road profiles. The four η-parameters characterizing the spline are selected via a minimax optimization problem whose solution can be obtained using a genetic/interval algorithm.

The proposed optimal spline appears as a motion planning primitive whose applicability, as far as curvature continuity is useful, may be also found for the planning of a broader class of nonholonomic vehicles.

Acknowledgements.

Partial support for this research has been provided by MURST and CNR scientific research funds.

References

[1] J. Ackermann. Robust car steering by yaw rate control. In *Proc. of the 1990 Conference on Decision and Control, CDC90*, pages 2033–2034, Honolulu, 1990.

[2] A. Broggi, M. Bertozzi, A. Fascioli, C. Guarino Lo Bianco, and A. Piazzi. The ARGO autonomous vehicle's vision and control systems. *International Journal of Intelligent Control and Systems*, 2000. to appear.

[3] R. H. Byrne, C. T. Abdallah, and P. Dorato. Experimental results in robust lateral control of highway vehicles. *IEEE Control Systems*, 18(2):70–76, 1998.

[4] B. Epiau, F. Chaumette, and P. Rives. A new approach to visual servoing. *IEEE Trans. on Robotics and Automation*, 8(3):313–326, 1992.

[5] R. Frezza, S. Soatto, and G. Picci. Visual path following by recursive spline updating. In *Proceedings of the 36th Conference on Decision and Control*, pages 1130–1134, San Diego, California USA, December 1997.

[6] C. Guarino Lo Bianco and A. Piazzi. A hybrid algorithm for infinitely constrained optimization. *International Journal of Systems Science*, 2000. to appear.

[7] T. Hessburg and M. Tomizuka. Fuzzy logic control for lateral vehicle guidance. *IEEE Contro System Magazine*, 14:55–63, August 1994.

[8] C.-C. Hsiung. *First Course in Differential Geometry*. Springer, New York (USA), 1998.

[9] Y. Ma, J. Košecká, and S. Sastry. Vision guided navigation for a nonholomonic mobile robot. *IEEE Transaction on Robotics and Automation*, 15(3):521–536, 1999.

[10] A. Piazzi and C. Guarino Lo Bianco. Quintic G^2-splines for trajectory planning of autonomous vehicles. In *Proceedings of the IEEE Intelligent Vehicles Symposium*, Dearborn, MI, October 2000.

[11] D. Pomerleau. RALPH: Rapidly adapting lateral position haldler. In *Proc. of the Int. Vehicles '95 Symposium*, pages 54–59, 1995.

[12] C. J. Taylor, J. Košecká, R. Blasi, and J. Malik. A comparative study of vision-based lateral control strategies for autonomous highway driving. *The International Journal of Robotic Research*, 18(5):442–453, 1999.

[13] S. Tsugawa, H. Mori, and S. Kato. A lateral control algorithm for vision-based vehicles with a moving target in the field of view. In *1998 International Conference on Intelligent Vehicles*, volume 1, pages 41–45, Stuttgart, Germany, Oct. 1999.